

# Advances in Space Research

## Development of Waterless Extra-Terrestrial Concrete Using Martian Regolith

--Manuscript Draft--

<b>Manuscript Number:</b>	
<b>Article Type:</b>	ST -Space Technology, Policy & Education
<b>Keywords:</b>	Martian regolith simulant; sulfur; microstructure; mineralogy; extreme temperature
<b>Corresponding Author:</b>	Piyush Chaunsali Indian Institute of Technology Madras Chennai, Tamil Nadu INDIA
<b>First Author:</b>	K Snehal
<b>Order of Authors:</b>	K Snehal Priyanshu Sinha Piyush Chaunsali
<b>Abstract:</b>	<p>Human colonization on Martian land is gaining significant attention in universal planetary exploration activities that demand in-situ resource utilization in the development of construction and building materials for human habitation. This research emphasizes the utilization of Martian regolith simulant to create extra-terrestrial concrete (ETC) with a property suitable for constructing human habitat on Mars. Mechanical, phase transition, and microstructure properties of Martian regolith based-ETC under varied temperature conditions (high: 40 °C and 50 °C; low: 0 °C) on Mars were investigated. The optimal mixture proportion of ETC had 70% of Martian regolith and exhibited a compressive strength of 27 MPa. The formulated ETC could retain up to 25 MPa of compressive strength under high (40 °C and 50 °C) and could reach up to 35 MPa under low (0 °C) temperature conditions. The change in compressive strength was attributed to the sulfur sublimation and pore closure brought on by freezing at high and low temperatures, respectively.</p>
<b>Suggested Reviewers:</b>	Gianluca Cusatis g-cusatis@northwestern.edu Expert in Space Concrete  Aloke Kumar alokekumar@iisc.ac.in Expertise in biocementation for space application  Faiz Shaikh S.Ahmed@curtin.edu.au Expert in concrete

# Development of Waterless Extra-Terrestrial Concrete Using Martian Regolith

Snehal K<sup>1</sup>, Priyanshu Sinha<sup>2</sup>, Piyush Chaunsali<sup>3#</sup>

<sup>1</sup>Department of Civil Engineering, MNNIT Allahabad, Prayagraj, India

<sup>2</sup>University of West England, BS16 1QY, United Kingdom

<sup>3</sup>Department of Civil Engineering, IIT Madras, Chennai, India

#Corresponding author: [pchaunsali@iitm.ac.in](mailto:pchaunsali@iitm.ac.in)

## Abstract

Human colonization on Martian land is gaining significant attention in universal planetary exploration activities that demand in-situ resource utilization in the development of construction and building materials for human habitation. This research emphasizes the utilization of Martian regolith simulant to create extra-terrestrial concrete (ETC) with a property suitable for constructing human habitat on Mars. Mechanical, phase transition, and microstructure properties of Martian regolith based-ETC under varied temperature conditions (high: 40 °C and 50 °C; low: 0 °C) on Mars were investigated. The optimal mixture proportion of ETC had 70% of Martian regolith and exhibited a compressive strength of 27 MPa. The formulated ETC could retain up to 25 MPa of compressive strength under high (40 °C and 50 °C) and could reach up to 35 MPa under low (0 °C) temperature conditions. The change in compressive strength was attributed to the sulfur sublimation and pore closure brought on by freezing at high and low temperatures, respectively.

**Keywords:** Martian regolith simulant, sulfur, microstructure, mineralogy, extreme temperature.

## 25 **1. Introduction**

26 Colonization of Mars has become an active target of space exploration since 20<sup>th</sup> century. Global  
27 public and private space organizations have set a goal for the settlement of human race on the red  
28 planet (Mars) by 2050 [Murgatroyd and Hodges, 2001; Scott et al., 2017]. One of the prime goals  
29 of the colonization effort is to maintain human life on the surface of Mars. Therefore, building a  
30 permanent and durable infrastructure for human inhabitation on Martian land has turned out to be  
31 the focus of research in universal planetary exploration activities [Jennifer et al., 2022]. The  
32 conveyance of building and construction materials from Earth to Mars is highly expensive and is  
33 going to be a challenging task. Instead, the most feasible approach is to use the indigenous  
34 resources as construction materials for building any permanent structures on Mars [Werkheiser, et  
35 al., 2015; Khoshnevis et al., 2016; Naser, 2019].

36 A research team from Northwestern University [Troemer et al., 2021] developed a novel way for  
37 making Martian concrete using naturally available materials on Mars. Rovers' data from NASA  
38 provides information that the red planet lacks liquid water but is found in a frozen state [NASA  
39 report 2022]. However, developed Martian concrete was designed without water, unlike the  
40 conventional concrete prepared on Earth [Troemer et al., 2021]. It is reported that planet Mars  
41 contains high levels of sulfur ( $\text{SO}_3$ ) concentration on its surface (approximately 37 wt%)  
42 [Scheerbaum, 2000]. The records also suggested a raised concentration of sulfur in the core [Rapp  
43 et al., 2006]. For that reason, the chief constituent considered in the development of Martian  
44 concrete is "sulfur", which acts as a binding material when heated to about 140 °C [Toutanji et al.,  
45 2005; Troemer et al., 2021]. Another possible constituent that is abundantly found on the red planet  
46 is "Martian soil" or "Martian regolith", which can be used as a source of aggregate. Martian  
47 concrete can be prepared by hot-mixing (using alternative sources of heating including solar  
48 energy) Martian regolith with molten sulfur, followed by casting and cooling [Toutanji et al., 2005;  
49 Troemer et al., 2021]. The phenomenon here is that once the mixture starts cooling, liquid sulfur  
50 initially crystallizes to monoclinic sulfur ( $\text{S}_\beta$ ) at 115 °C, and further cooling below 96 °C transforms  
51 to orthorhombic sulfur ( $\text{S}_\alpha$ ) [Wan et al., 2016].  $\text{S}_\alpha$  is a stable form of sulfur at room temperature.  
52 This solidification process of liquid sulfur takes place quickly, i.e., within 24 hours, binding the  
53 regolith strongly to produce a rapid-hardening construction material. In the case of waterless  
54 Martian concrete, sulfur functions as a thermo-plastic material with the ability to hold the non-  
55 reactive Martian regolith together [Toutanji et al., 2008]. The major advantage of Martian concrete

56 over Earth's concrete is that this concrete can be reused by reheating until sulfur melts and gets  
57 back to a malleable state. Apart from this fact, it is also a carbon-neutral construction material,  
58 unlike cement concrete on Earth. Researchers have used Martian regolith simulants (mixture of  
59  $\text{TiO}_2$ ,  $\text{Fe}_2\text{O}_3$ ,  $\text{SiO}_2$ ,  $\text{Al}_2\text{O}_3$ , and other constituents) with a proportion nearly similar to actual Martian  
60 regolith [Toutanji et al., 2005; Toutanji et al., 2008; Troemer et al., 2021]. They were able to  
61 fabricate the Martian concrete blocks (with a compressive strength of 50 MPa), which are two and  
62 a half times stronger than the Earth's conventional concrete, using 50% martial soil simulant and  
63 50% molten sulfur [Troemer et al., 2021].

64 Several other approaches considered for extraterrestrial construction are conventional OPC  
65 concrete formulated with regolith as aggregate [Neves et al., 2020], epoxy/polymer-based binder  
66 cement [Naser, 2019; Naser and Chehab, 2020] and alkali activate/geopolymer binder system  
67 [Montes et al., 2015; Davis et al., 2017; Pilehvar et al., 2020; Zhou et al., 2020]. The  
68 epoxy/polymer-based binder system requires supplementary earthly resources for the bulk of the  
69 binder [Naser, 2019; Naser and Chehab, 2020]. While researchers have demonstrated the  
70 possibility of producing geopolymer binders using extraterrestrial regolith simulant itself.  
71 However, to produce a geopolymer binder it is required to dissolve and activate regolith rich in  
72 aluminosilicate minerals and that necessitates some solution/activator [Montes et al., 2015;  
73 Pilehvar et al., 2020]. Even though sulfur is not an abundantly available material on the Lunar  
74 surface, the sulfur-based binder may serve as an appropriate binder material for Martian  
75 constructions owing to its abundancy on the Martian surface [King and McLennan, 2010;  
76 Khoshnevis et al., 2016].

77 Landers and rovers from NASA successfully discovered that partial Martian conditions such as  
78 day length, seasons, and surface conditions match with Earth [NASA report 2022]. However, Mars  
79 has a much thinner, colder, and low gravity atmosphere versus Earth. Near the poles, the  
80 temperature can drop up to  $-125\text{ }^\circ\text{C}$  during winter, and near the equator, temperature may reach up  
81 to  $20\text{ }^\circ\text{C}$  during summer. Nevertheless, night temperature can fall to about  $-73\text{ }^\circ\text{C}$  [Scheerbaum,  
82 2000]. Therefore, building infrastructure on Mars is an engineering challenge [Jennifer et al.,  
83 2022]. Following this fact, it is important to understand the behavior of Martian concrete  
84 formulated using Martian regolith and sulfur ingredient at extreme temperature cycles of Mars.  
85 However, a very few studies focused on the performance of Martian concrete under extreme  
86 temperature conditions of Mars. In this study, at first, Martian regolith concrete was prepared using

87 the varied proportion of Martian regolith simulant and sulfur to determine the optimum mix in  
 88 correspondence to compressive strength. Then, the performance and transformation in the  
 89 microstructure of produced Martian regolith simulant-based ETC under extreme temperature  
 90 conditions were investigated. The microstructure of Martian concrete before and after exposure to  
 91 varied climatic temperature of Mars at the laboratory were evaluated using characterization  
 92 techniques such as quantitative Xray diffraction (QXRD), thermogravimetric analysis (TGA),  
 93 Fourier-transform Infrared spectroscopy, and Scanning Electron Microscope (SEM).

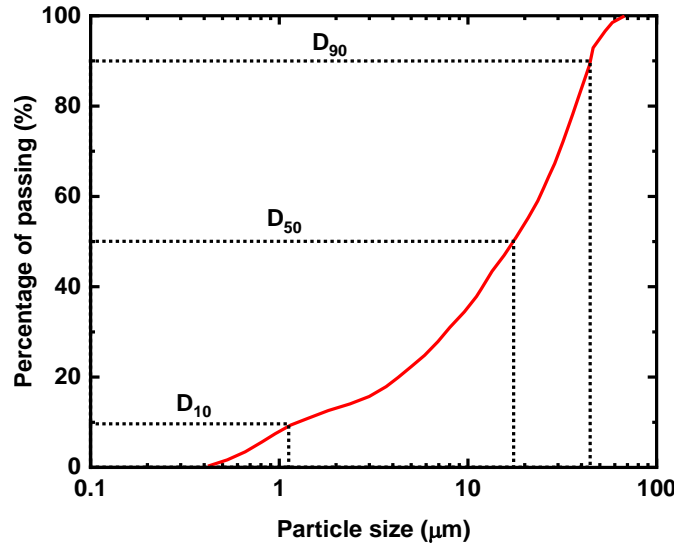
94 **2. Experimental investigation**

95 *2.1 Materials*

96 A Martian regolith simulant (MGS-1) procured from the Exolith Lab (Florida, USA) and  
 97 commercially available 99.8% pure sulfur powder were used in this work. The oxide composition  
 98 and specific gravity value of the MGS-1 are given in the Table. 1. The major components of  
 99 Martian soil are SiO<sub>2</sub>, Al<sub>2</sub>O<sub>3</sub>, and Fe<sub>2</sub>O<sub>3</sub>, which account for more than 75% of the overall oxide  
 100 composition. The particle size distribution curve of MGS-1 is shown in Fig. 1. The D<sub>10</sub>, D<sub>50</sub>, and  
 101 D<sub>90</sub> values of the Martian regolith simulants are found to be 1.07 μm, 17.5 μm, and 43.8 μm,  
 102 respectively.

103 Table 1 Oxide composition and specific gravity value of the MGS-1.

Oxide composition (wt%)	
SiO <sub>2</sub>	44.2414
Al <sub>2</sub> O <sub>3</sub>	13.4357
Fe <sub>2</sub> O <sub>3</sub>	20.9348
SO <sub>3</sub>	5.9177
CaO	7.3779
Na <sub>2</sub> O	0.5706
MgO	6.3571
K <sub>2</sub> O	0.5256
Cl	0.0229
Cr <sub>2</sub> O <sub>3</sub>	0.2381
MnO	0.1384
NiO	0.1772
SrO	0.0628
Specific gravity	2.83

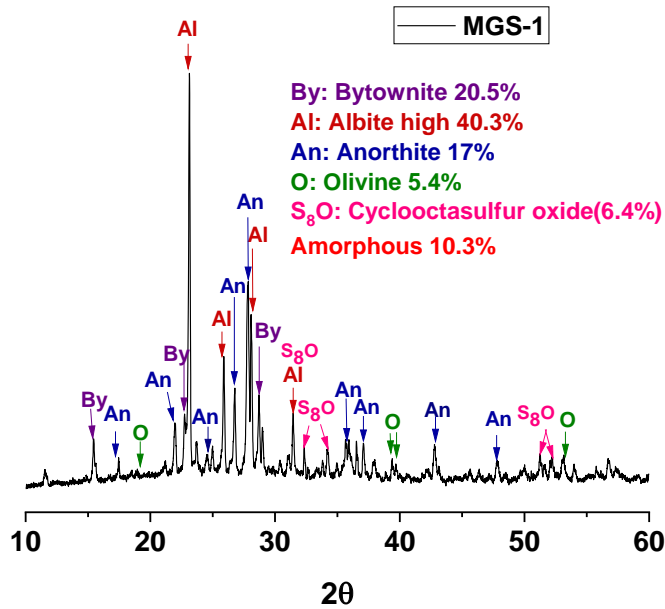


104

Fig. 1. Particle size distribution of Martian regolith simulant (MGS-1).

105

106 X-ray diffraction (XRD) pattern, thermogravimetric (TG-DTG) curve, and scanning Electron  
 107 micrograph (SEM) with energy dispersive spectroscopic (EDS) information of MGS-1 are shown  
 108 in Figs. 2-4, respectively.



109

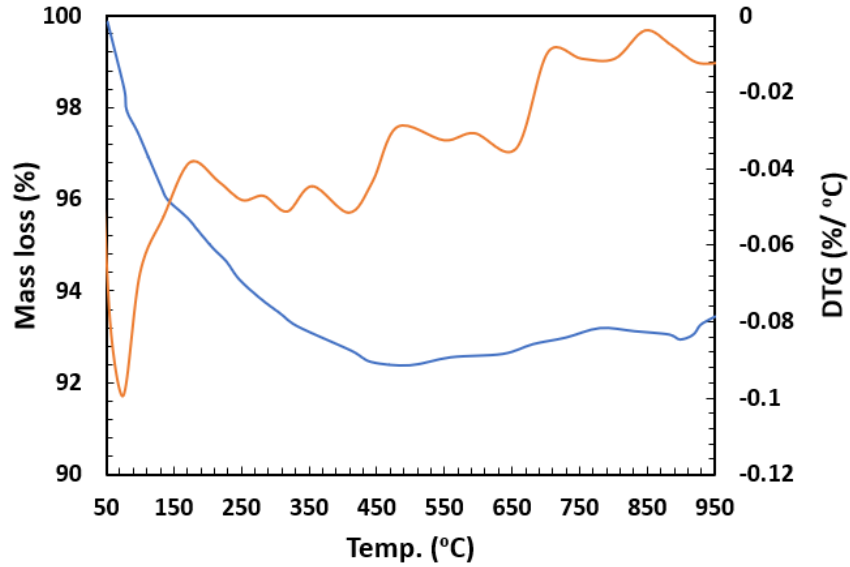
Fig. 2. XRD pattern of Martian regolith simulant (MGS-1).

110

111

112

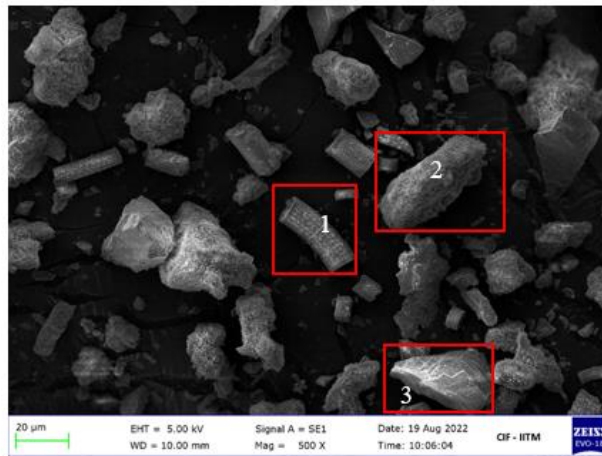
113



114

115

Fig. 3. TG-DTG curve of Martian regolith simulant (MGS-1).



116

117

Fig. 4. Morphology of Martian regolith simulant (MGS-1).

118

Table 2 Elemental composition of Martian regolith simulant (MGS-1).

Point (morphology)	Si	Al	O	C	Na	Mg	S	Ca	Fe	K	Mineral phases
	Atomic weight %										
1 (Perforated tube)	23.89	1.37	70.82	-	-	1.23	1.68	0.25	0.69	0.07	Olivine: $MgFe_2SiO_4$ Anorthite: $CaAl_2Si_2O_8$
2 (Smooth irregular)	16.75	6.98	64.57	-	4.58	2.48	0.58	2.52	-	0.33	Anorthite: $CaAl_2Si_2O_8$ Albite: $NaAlSi_3O_8$
3 (angular)	16.37	14.62	57.26	2.37	2.15	-	-	6.94	-	-	Anorthite: $CaAl_2Si_2O_8$ Albite: $NaAlSi_3O_8$ Bytownite: $(Ca,Na)[Al(Al,Si)SiO_8]$

119 According to XRD pattern (Fig. 2), albite ( $\text{NaAlSi}_3\text{O}_8$ ), anorthite ( $\text{CaAl}_2\text{Si}_2\text{O}_8$ ), bytownite  
 120 ( $(\text{Ca},\text{Na})[\text{Al}(\text{Al},\text{Si})\text{SiO}_8]$ ) and olivine ( $\text{MgFe}_2\text{SiO}_4$ ) are the most common minerals observed in  
 121 Martian regolith simulant (MGS-1). The thermogravimetric analysis (TGA) of MGS-1 (Fig. 3)  
 122 revealed multiple endothermic and exothermic peaks associated with the decomposition of glass  
 123 phases. It is reported that endothermic peaks corresponding to the decomposition of major mineral  
 124 phases such as albite, olivine, etc., are noticed at the temperature range of 1000-1600 °C. The  
 125 complete decomposition of mineral phases of MGS-1 was not recorded in the TG analysis, since  
 126 the MGS-1 possesses its characteristic decomposition temperature above 1000°C. However, MGS-  
 127 1 exhibited a mass loss of about 9% till the maximum recorded temperature of 950 °C. SEM  
 128 micrographs of MGS-1 (Fig. 4) illustrated a complex structure with three major morphologies, i.e.,  
 129 1) perforated tubular structure (Olivine:  $\text{MgFe}_2\text{SiO}_4$ ) smooth irregular structure (Albite:  
 130  $\text{NaAlSi}_3\text{O}_8$ ; Olivine:  $\text{MgFe}_2\text{SiO}_4$ ), and 3) angular structure (Anorthite:  $\text{CaAl}_2\text{Si}_2\text{O}_8$ ; Albite:  
 131  $\text{NaAlSi}_3\text{O}_8$ ; Bytownite:  $(\text{Ca},\text{Na})[\text{Al}(\text{Al},\text{Si})\text{SiO}_8]$ ). Table 2 presents the elemental composition of  
 132 various morphologies observed in the Martian regolith simulant (MGS-1).

133 *2.2 Preparation of Martian regolith simulant-based ETC*

134 Martian regolith simulant-based ETC specimens were cast in varying proportions of Martian  
 135 simulant and sulfur. Table 3 shows various mix proportions of waterless Martian concrete used in  
 136 the study.

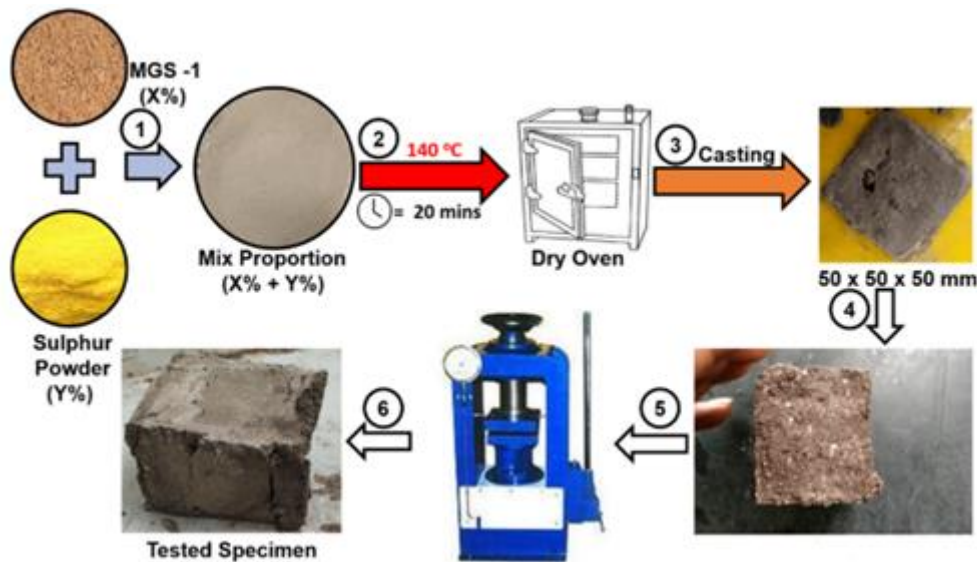
137 Table 3 Mix proportion of Martian concrete.

Mix designations	MGS-1(%)	Sulfur (%)
MC-75/25	75	25
MC-73/27	73	27
MC-70/30	70	30
MC-65/35	65	35

138 Martian concrete was synthesized by blending both Martian simulant and sulfur powder at various  
 139 proportions as mentioned in Table 3. It is important to note that the agglomeration of the sulfur  
 140 particle was removed during the process of mixing. Next, the uniformly spread blended samples  
 141 placed on the metal tray were kept in the oven and maintained at 140 °C for about 20 mins. Interval  
 142 mixing (every 5 min) was performed to ensure the consistency of paste. Then, the tray was taken  
 143 out of the oven and the paste was placed in the acrylic mould of size 50 × 50 × 50 mm and was



144 compacted using a wooden block. After 24 hours, the specimens were de-moulded and tested for  
145 compressive strength. Fig. 5 shows the process of producing Martian concrete.



146

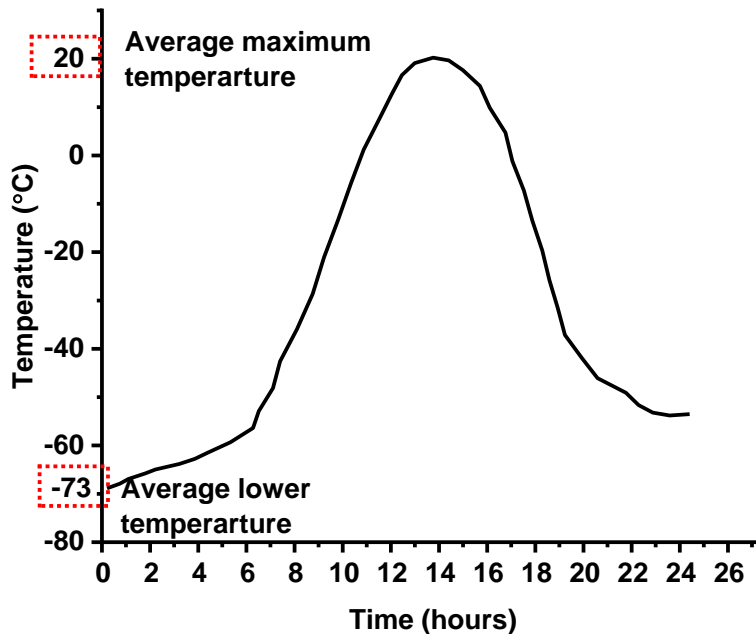
147

Fig. 5. Process of producing Martian concrete.

148 After that laboratory-scale tests were conducted on the Martian concrete specimens on exposing  
149 to extreme temperature conditions.

### 150 2.3 Laboratory scale test on extreme temperature conditions

151 Due to the thinner, colder, and low gravity atmosphere of Mars, buildings on the Martian surface  
152 would suffer extreme temperature cycles and thermal shocks. The temperature on the Martian  
153 surface may reach up to 20 °C at noon and drops to -73 °C at night during summer near the equator.  
154 However, the temperature may reach up to -125 °C during winter near the poles [Scheerbaum,  
155 2000]. A typical variation of temperature on the Martian surface is shown in Fig. 6.



156

157 Fig. 6. Typical temperature variation curve on the Martian surface as per Mars exploration Rover  
 158 data of NASA [www.nasa.gov].

159 To assess the behavior of Martian regolith simulant-based ETC under extreme temperatures,  
 160 experiments were conducted considering the high and low-temperature tests at the laboratory scale.  
 161 Temperature resistance tests of Martian regolith simulant-based ETC were carried out under  
 162 different temperatures such as 50 °C, 40 °C, and 0 °C. Specimens exposed to different temperatures  
 163 for the duration of 7 and 28 days were tested for compressive strength.

164 *2.4 Test methods*

165 *2.4.1 Compressive strength*

166 The compressive strength test of Martian concrete specimens was conducted as per IS 4031 Part-  
 167 6. Specimens were tested using a hydraulic compression testing machine of capacity 250 kN at the  
 168 loading rate of 35 N/mm<sup>2</sup>/min. The average of three specimens was recorded as compressive  
 169 strength of concrete.

170 *2.4.2 X-ray diffraction (XRD)*

171 X-ray diffraction was used to characterize the mineralogical composition of Martian concrete  
 172 exposed to high and low-temperature environment. XRD pattern of fine powdered samples  
 173 (passing through 75 µm sieve) was obtained through MiniFlex Rigaku powder X-ray diffraction

174 instrument operated with Cu K $\alpha$  radiation (40 kV/40 mA). The scanning speed, step size, and  
175 deflection angle ( $2\theta$ ) were all kept constant at 2°/min, 0.01° and 10° to 70°, respectively.  
176 Quantitative analysis of XRD data was performed using X'Pert High Score Plus software allied  
177 with Rietveld analysis.

#### 178 *2.4.3 Thermogravimetric analysis (TGA)*

179 Thermogravimetric analysis (TGA) was carried out for powdered samples passing through 75  $\mu\text{m}$   
180 sieve using FEI-Quanta FEG 200F. Samples were heated to a temperature of 35-950 °C (heating  
181 rate: 10 °C/min) in a nitrogen purge environment (flow rate: 20 ml/min). TGA was done on samples  
182 that were exposed to various temperatures for the period of 7 and 28 days.

#### 183 *2.4.4 Fourier-transform infrared spectroscopy (FTIR)*

184 Fourier-transform infrared spectroscopy (FTIR) was used to identify the change in the functional  
185 group of Martian concrete s. The FTIR spectroscopy was performed on powdered samples that  
186 had passed through a 75  $\mu\text{m}$  sieve. FTIR spectra were obtained from Bruker (Alpha II) FTIR  
187 equipment at the wavenumber range of 1650 to 600  $\text{cm}^{-1}$  with a resolution of 2  $\text{cm}^{-1}$  and at 32  
188 scans. Attenuated total reflection (ATR) sampling mode was used to run the samples.

#### 189 *2.4.5 Scanning electron microscopy (SEM) and energy-dispersive X-ray spectroscopy (EDS)*

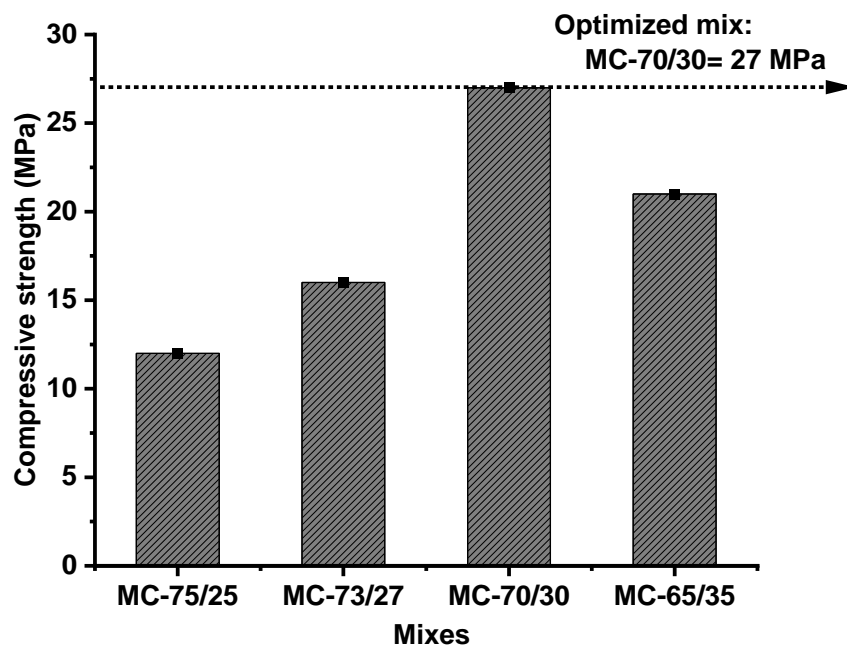
190 Chunks of the crushed sample were vacuum dried and gold-sputtered to analyze the  
191 microstructure. A JEOL, JSM-638OLA, scanning electron microscope (SEM) was used for  
192 characterizing the morphological characteristics of Martian concrete samples.

193

194 **3 Results and discussion**

195 *3.1 Compressive strength of Martian regolith simulant-based ETC*

196 Extra-terrestrial concrete (ETC) was developed on Earth using Martian regolith. Fig. 7 shows the  
197 compressive strength of ETC after 24 hours. It can be seen that the compressive strength of Martian  
198 concrete gradually increased with the increase in the binder content, i.e., sulfur up to a certain  
199 limit. Specimens with 70% Martian regolith simulant and 30% sulfur content attained the  
200 compressive strength of 27 MPa in 24 hours. Further increase in sulfur content to 35% showed a  
201 reduction in compressive strength i.e., 21 MPa. This could be attributed to the increased level of  
202 crystallinity brought about by the cooling-induced crystallization of sulfur. It is reported that the  
203 compressive strength of Martian simulant-based composite depends on the particle size of the  
204 regolith and the crystallization of sulfur [Wan 2016]. Finer particle size and well-graded Martian  
205 regolith contribute to the more compacted Martian concrete. The sulfur as well as sulfate/poly-  
206 sulfate phases engendered from the ample metals existing in the Martian regolith also add to the  
207 strength of Martian concrete.



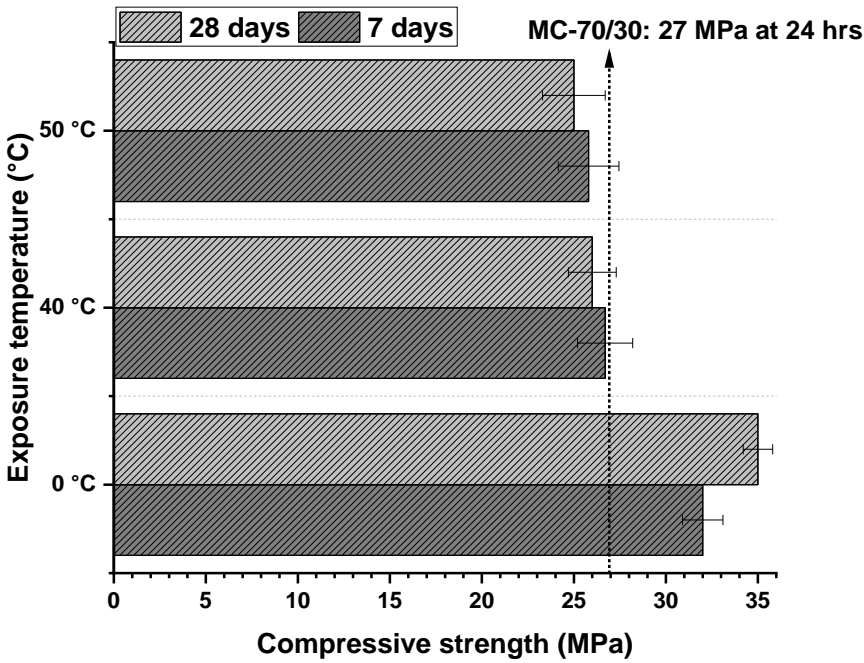
208  
209 Fig. 7. Compressive strength of ETC containing Martian regolith simulant after 24 hours.

210 Even though mechanical characteristics are sufficient to satisfy the building requirements on the  
211 Martian surface, the mechanical properties of ETC under Martian environment are not well-  
212 explored. The optimal proportion (based on compressive strength) of Martian regolith simulant

213 and sulfur content for producing a waterless Martian concrete was found to be 70% and 30%,  
214 respectively (Fig. 7). In the next stage, the optimized ETC was studied for its mechanical and  
215 microstructural characteristics at Martian surface temperature condition.

216 *3.2. Compressive strength of Martian regolith simulant-based ETC under high and low-*  
217 *temperature conditions*

218 Compressive strength of ETC containing Martian regolith simulant exposed to high (40 °C and 50  
219 °C) and low (0 °C) for the period of 7 and 28 days is presented in Fig. 8.



220  
221 Fig. 8. Compressive strength of ETC containing Martian regolith simulant at varied temperature  
222 condition.

223 From Fig 8, it can be seen that at high temperature of 40 °C and 50 °C, compressive strength of  
224 Martian concrete had little effect, and values were found to be reduced by 1% to 4% at 7 days of  
225 exposure and 3% to 7% at 28 days of exposure, respectively. However, the compressive strength  
226 of designed Martian regolith simulant-based ETC could able to maintain the nominal concrete  
227 strength of 25 MPa under the temperature of 40 °C to 50 °C. It is important to note that melting of  
228 sulfur takes place at the temperature of 120 °C, while the temperature on the Martian surface near  
229 equator can reach up to 20-30 °C. Therefore, sulfur-based Martian concrete is less susceptible to  
230 Martian surface temperature. According to Grugel et al. (2016), sulfur sublimation occurs at a high

231 temperature of 120 °C over two hours, and the rate of sublimation increases significantly as the  
232 temperature rises. At the same time, it was also estimated to take 3.7 years to submilate 1 cm layer  
233 of sulfur at 15 °C due to the the impact of lower lunar pressure [Grugel et al. 2008; Grugel et al.,  
234 2016]. In this concern, sulfur-based lunar regolith composite is not an ideal approach for lunar  
235 constructions as the temperature on Moon reaches 120 °C near the equator. However, this might be  
236 one of the most ideal solutions for developing infrastructure on Mars.

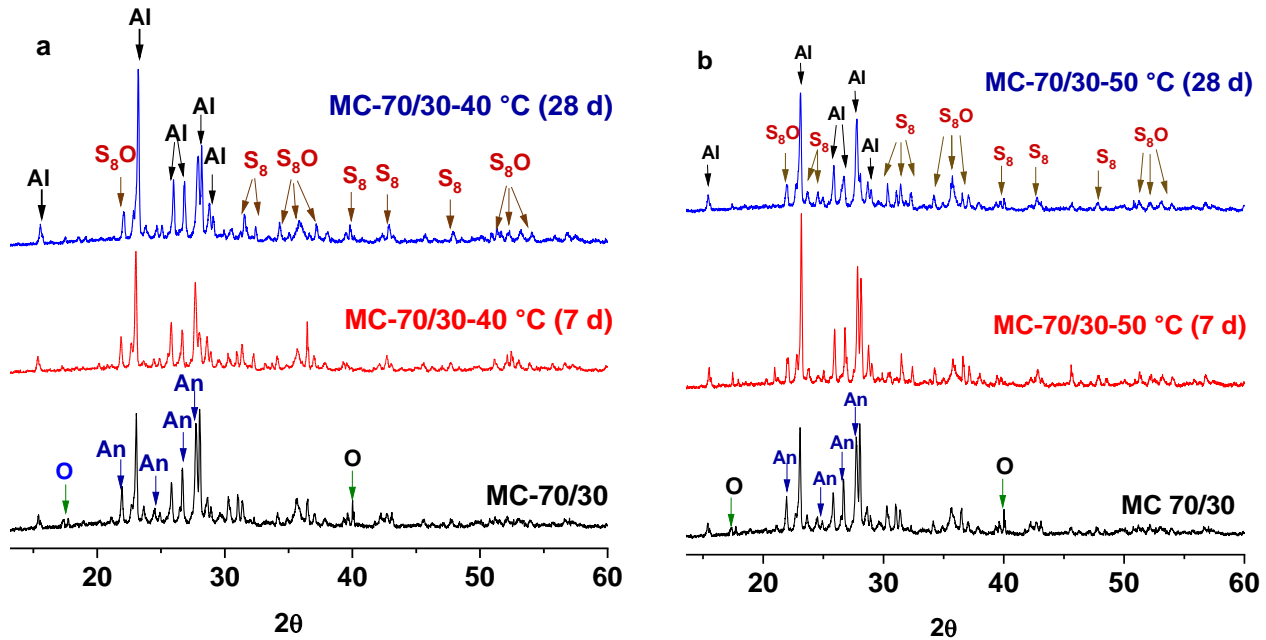
237 As seen in Fig. 8, the compressive strength of Martian concrete, when exposed to low temperatures  
238 of 0°C, can reach up to 35 MPa after 28 days, surpassing that of the reference specimen (MC70/30).  
239 This is due to closing of pores in the Martian concrete as a result of freezing activity [Montejo et  
240 al., 2008]. The strength increases as the ice strength increases with the drop in temperature.  
241 Therefore, it is understood that Martian regolith simulant-based ETC performs better in terms of  
242 compressive strength at low-temperature conditions.

### 243 *3.3 Mineralogical and phase transformation properties of Martian regolith simulant-based ETC* 244 *exposed to high and low-temperature conditions*

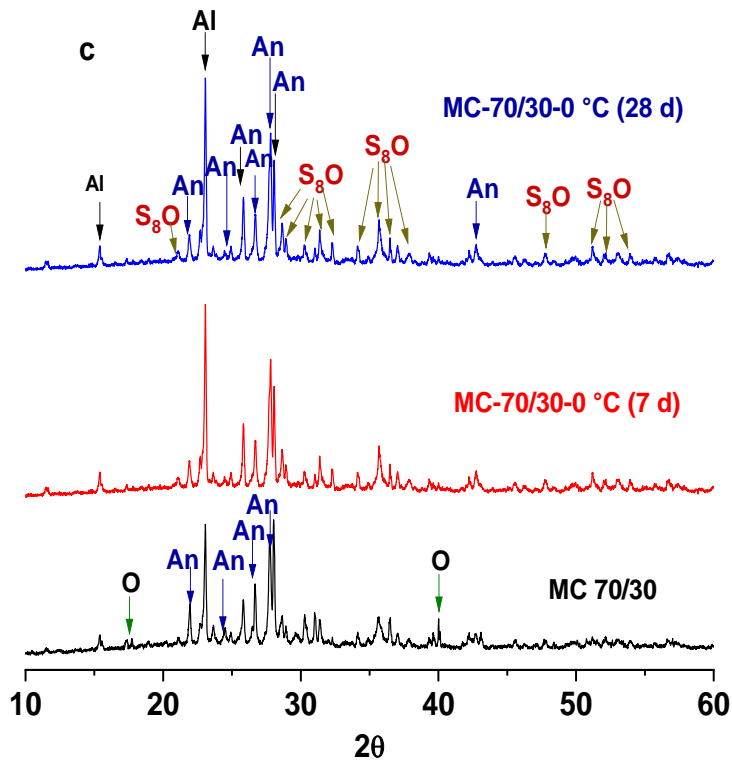
245 Variation in the mineralogical composition of Martian concrete exposed to different temperature  
246 conditions was monitored using XRD. Fig. 9 displays the XRD patterns of Martian concrete  
247 exposed to 40°C, 50°C, and 0°C for 7 and 28 days.

248

249



250



251 Fig. 9. XRD patterns of Martian concrete exposed to a) 40 °C, b) 50 °C, and c) 0 °C for 28 days.

252 Anorthite (An), albite (Al), and olivine (O) are the three main mineral phases seen in the Martian  
 253 concrete, these phases were also evident in the Martian regolith simulant. In addition to that,  
 254 cyclooctasulfur oxide (S<sub>8</sub>O) and octasulfur (S<sub>8</sub>) phases are noticed in Martian concrete at higher

255 percentage than Martian regolith simulant. Bytownite, a plagioclase mineral observed in Martian  
 256 regolith simulant, was found to be changed to anorthite (An) phase when heated with sulfur to create  
 257 Martian concrete. Bytownite is composed of 80–90% anorthite and 10–20% albite. After exposure to  
 258 40 °C and 50 °C anorthite phases were seen to be replaced by albite phase at both 7 and 28 days of  
 259 exposure (Fig. 9 a-b). It is reported that sulfur sublimates (i.e., phase change of sulfur from solid to  
 260 gas without transitioning through a liquid state) in the temperature range of 25 °C to 50 °C and this  
 261 phase transition leaves the structure of the S<sub>8</sub> ring unaltered [Nash, 1987].

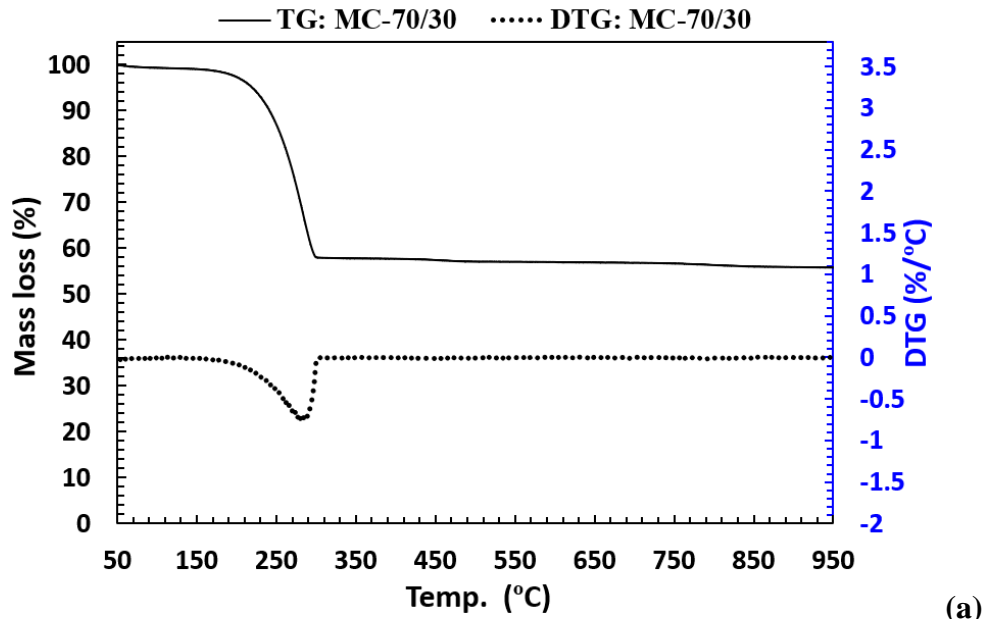
262 At 0 °C, all mineral phases remained the same as they were at MC-70/30 (without exposure to  
 263 temperature), in contrast to the Martian concrete specimens exposed to 40 °C and 50 °C (Fig. 9c).  
 264 However, in all exposed temperature conditions, i.e., 40 °C, 50 °C, and 0 °C, the olivine (O) phase  
 265 was observed to have disappeared. Quantitative X-ray diffraction (QXRD) analysis was used to  
 266 determine the fraction of mineral phases formed in Martian concrete when exposed to varied  
 267 temperature conditions and the same has been listed in Table 4.

268 Table 4 Phase composition of Martian regolith simulant-based ETC exposed to 40 °C, 50 °C, and 0  
 269 °C to the duration of 7 and 28 days.

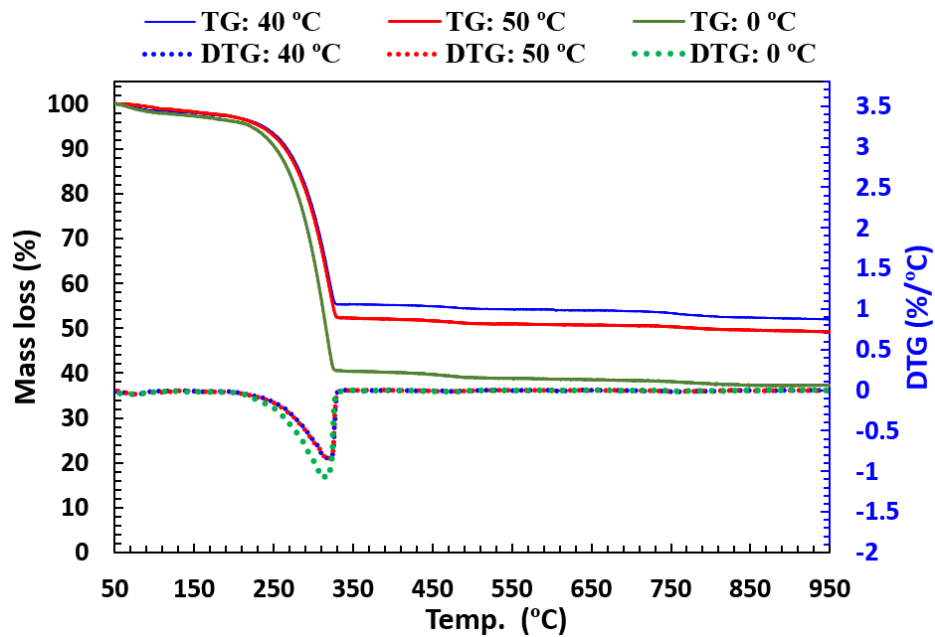
Phase composition	MC-70/30						
	Before exposure	40 °C		50 °C		0 °C	
		7 days	28 days	7 days	28 days	7 days	28 days
Cyclooctasulfur oxide (S <sub>8</sub> O)	16.7%	17.7%	19.5%	12.65%	18.9%	26.2%	29.2%
Albite (Al)	26.7%	29.3%	27.2%	37.4%	32.9%	16.1%	8.8%
Octa sulfur (S <sub>8</sub> )	-	13.3%	14.9%	20.0%	22.2%	-	-
Anorthite (An)	4.2%	-	-	-	-	21.7%	17.2%
Olivine (O)	3.8%	-	-	-	-	-	-

270 To evaluate the phase transformation of Martian regolith simulant-based ETC before and after exposure  
 271 to 40 °C, 50 °C, and 0 °C, thermogravimetric analysis was performed at 7 and 28 days of exposure  
 272 time. For brevity, TG-DTG plot of Martian regolith simulant-based ETC (MC-70/30) before and after  
 273 28 days of temperature exposure is illustrated in Fig. 10.





(a)



(b)

274

275 Fig. 10. TG-DTG curve of Martian regolith simulant-based ETC to a) MC-70/30 b) MC-70/30

276

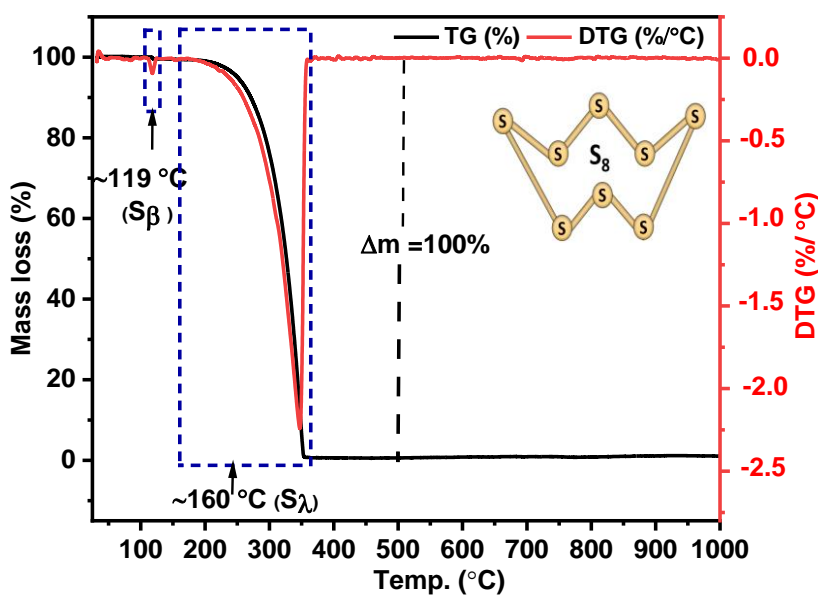
after exposure to 40 °C, 50 °C, and 0 °C for 28 days.

277

Table 5 Thermogravimetric mass loss percentage at  $\lambda$ -transition temperature of sulfur.

Mix designation		Temperature boundary ( $\lambda$ -transition)	Mass loss (%)
MC-70/30		193-312 °C	40.65
MC-70/30-40 °C	7 days	166-350 °C	41.27
	28 days	166-350 °C	42.05
MC-70/30-50 °C	7 days	166-350 °C	43.77
	28 days	166-350 °C	45.57
MC-70/30-0 °C	7 days	193-322 °C	41.06
	28 days	193-322 °C	55.48

279 The major endothermic peak was noticed at the temperature boundary of 193-312 °C for MC-70/30  
 280 (Fig. 10). When Martian concrete was exposed to temperatures of 40 °C and 50 °C (Fig. 10a-b),  
 281 the same endothermic peak was found to be broadened. The onset and end temperatures for the  
 282 Martian concrete exposed to high (40 °C and 50 °C) and low (0 °C) temperatures were measured  
 283 to be 166-350 °C and 193-322 °C, respectively. This endothermic peak corresponds to the  
 284 decomposition of sulfur components in the Martian concrete. Generally, pure sulfur ( $S_8$ ) begins to  
 285 evaporate at roughly 160 °C, grows gradually to reach its maximum between 200-300 °C, and then  
 286 ends at around 330-350 °C. TG-DTG plot of pure sulfur used in the study is illustrated in Fig. 11.



287

288

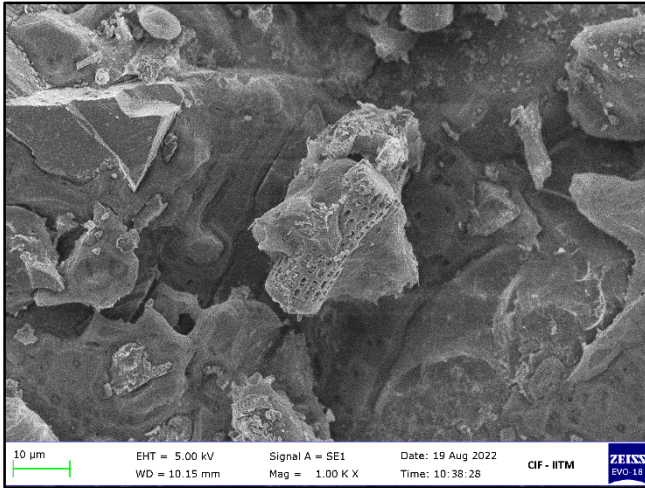
Fig. 11. TG-DTG curve of pure sulfur.

289 Understanding the phase transformation of sulfur requires knowledge of the allotropic forms of  
290 the element. Orthorhombic  $\alpha$ -sulfur ( $S_\alpha$ ), monoclinic  $\beta$ -sulfur ( $S_\beta$ ), and monoclinic  $\gamma$ -sulfur ( $S_\gamma$ )  
291 are the three most prevalent allotropes found in cyclo-octa sulfur ( $S_8$ ) [Steudel, 2003]. All the  
292 cyclo-octa sulfur allotropes have puckered rings of  $S_8$  with different spatial arrangements [Norman  
293 and Alan 1997].  $\alpha$ -sulfur ( $S_\alpha$ ) is the thermodynamically stable form of sulfur at ambient conditions  
294 ( $<96$  °C) and a temperature above 96 °C the  $S_\alpha$  sulfur changes to the monoclinic  $\beta$ -sulfur ( $S_\beta$ )  
295 [Norman and Alan 1997]. Melting of  $S_\beta$  sulfur takes place at approximately 115 °C that is revealed  
296 by a small endothermic peak in DTG curve (Fig. 11). However,  $S_\beta$  is metastable and can transform  
297 back into  $S_\alpha$  when the temperature drops below 96 °C [Wan et al., 2016].  $S_\gamma$  sulfur is the densest  
298 allotrope of  $S_8$  sulfur, which is formed when molten sulfur (heated above 150 °C) is quenched by  
299 chilling solutions [Steudel, 2003], this transformation is not observed in Fig. 11. A significant  
300 endothermic peak noticed at the temperature of  $\sim 160$  °C is associated to the transition of  $\lambda$ - sulfur  
301 ( $S_\lambda$ ) (Fig. 11) [Eilene, 1982]. After melting of  $S_\beta$  sulfur, rings of  $S_8$  get converted to linear  
302 polymeric bi-radical molecules ( $-S-S_6-S-$ ) in the temperature range of about 160-350 °C, which is  
303 indicated by an endothermic reaction called  $\lambda$ -transition [Carotenuto et al., 2013]. In the case of  
304 pure sulfur, 100% mass loss has been recorded at the temperature range of 160-350°C indicating  
305 the complete decomposition of sulfur.

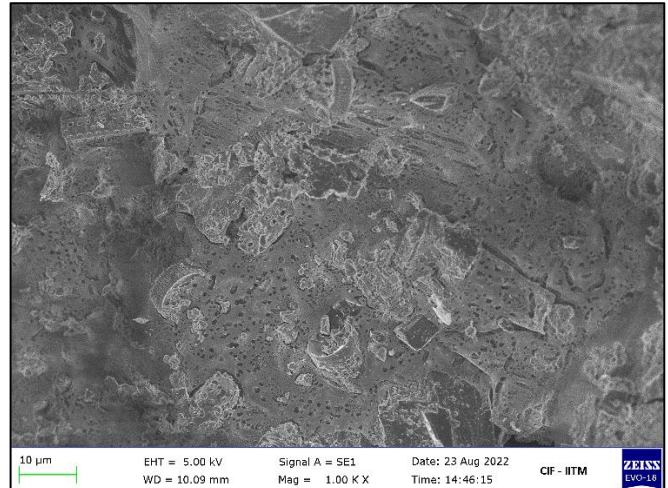
306 It can be seen from Fig. 10 and Table 5 that the total mass loss of ETC resulted from the  
307 vaporization of sulfur stored in the pores of the matrix is measured to be 40.65% (at the temperature  
308 range of 193-312 °C). Further, it is important to note that the mass loss of ETC subjected to 40 °C,  
309 50 °C, and 0 °C for 28 days was found to be increased to 42%, 45%, and 55%, respectively (Table  
310 5). The mass loss of ETC associated to the  $\lambda$ -transition temperature of sulfur was recorded at the  
311 temperature boundaries of 166-350 °C (for 40 °C and 50 °C exposed samples) and 193-322 °C (for  
312 0 °C exposed samples). Even though proportioned ETC comprised only 30% of sulfur content, the  
313 increased percentage of sulfur in ETC recorded from TGA quantification could be attributed to the  
314 additional sulfur composition present in Martian regolith simulant (Fig. 2).

### 315 *3.4 Morphological characteristics*

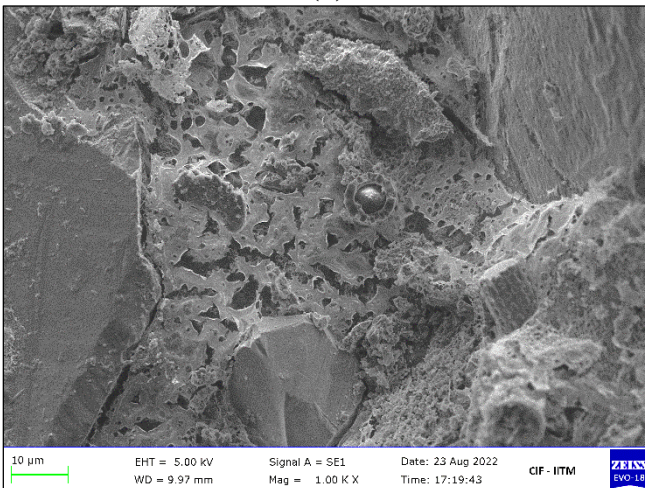
316 The morphology of Martian concrete before and after exposing to 40 °C, 50 °C, and 0 °C for 28  
317 days are shown in Fig. 11



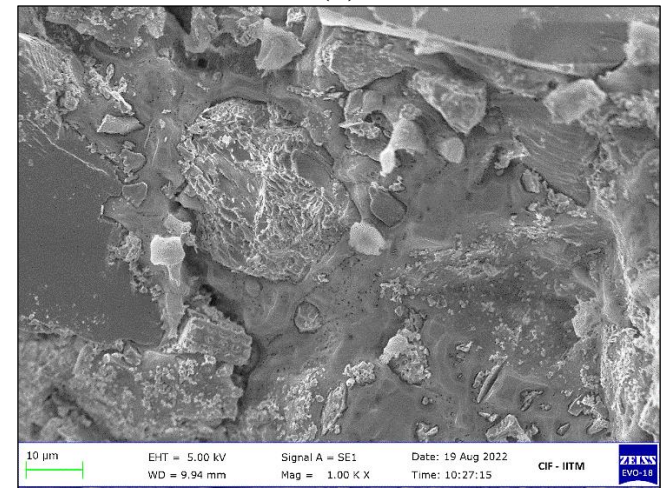
(a)



(b)



(c)



(d)

318 Fig. 11. Morphology of ETC exposed to a) before exposure b) 40 °C to 28 days c) 50 °C to 28  
 319 days and d) 0 °C to 28 days flocculates.

320 There are no obvious large defects in the internal structure observed in ETC after exposure to 40  
 321 °C and 50 °C, as evident in Figure 11. Morphology of ETC tends to get porous when exposed 40  
 322 °C and 50 °C. This can be ascribed to the sublimation and disintegration of the sulfur phase in the  
 323 matrix of ETC (Fig. 11b and Fig.11c). This could be one of the probable reasons for the reduction  
 324 in compressive strength of ETC under 40 °C and 50 °C. While Fig. 11d shows a more dense and  
 325 homogenous morphology with filled pores in the matrix. This may be attributed to the pores filled  
 326 due to the freezing activity at a low temperature of 0 °C and thereby contributes to the enhancement  
 327 in the strength performance of ETC.

328 The temperature and pressure condition are the important features that affects the robustness of

329 ETC made up of sulfur. Grugel and Toutanji (2008) observed significant formation of pores and  
330 flaws in sulfur based lunar concrete at 120 °C due to the sublimation of sulfur ( $S_{\beta}$ : monoclinic  
331 sulfur) at high temperature ( $>115$  °C). However, maximum temperature on the Mars near equator  
332 would be 30 °C, where sublimation of sulfur is inconsequential and takes place at a slow pace  
333 (NASA.gov). Durability of ETC made up of sulfur is significantly influenced by the temperature  
334 cycle on Mars as well. Solidification of ETC takes place by the process of cooling crystallization  
335 of sulfur. It is reported that transformation of  $S_{\lambda}$  to  $S_{\beta}$  sulfur when temperature drops to 115 °C and  
336  $S_{\beta}$  to  $S_{\alpha}$  at 96 °C may lead to the volumetric changes in sulfur causing variation in the microstructure  
337 of ETC (Wan et al., 2016). In our current work, controlling hardening of Martian regolith simulant-  
338 based ETC was challenging. Future research should be directed to explore additives to control the  
339 hardening rate of this type of ETC.

#### 340 **4. Conclusions**

341 In this study Martian concrete was produced using Martian regolith simulant as aggregate and  
342 sulfur as a binding ingredient. Emphasis has been given to understanding the disparity in  
343 mechanical, mineralogical, phase transition, and morphological properties of Martian concrete  
344 under the varied temperature conditions (40 °C, 50 °C, and 0 °C). Based on the study following  
345 conclusions were drawn:

- 346 • The Martian concrete proportioned with 70% Martian regolith simulant and 30% sulfur  
347 achieved the optimal compressive strength of 27 MPa at 24 hours as a result of the molten sulfur  
348 crystallization phenomenon at ambient temperature.
- 349 • Phases belonging to feldspar families such as anorthite ( $CaAl_2Si_2O_8$ ), albite ( $NaAlSi_3O_8$ ), and  
350 olivine ( $MgFe_2SiO_4$ ) are the three main mineral phases seen in the ETC, similar to Martian  
351 regolith simulant. In addition to that, cyclooctasulfur oxide ( $S_8O$ ) and octasulfur ( $S_8$ ) phases  
352 were also noticed at higher percentage in ETC.
- 353 • The slow and low sublimation of sulfur at the temperature of 40 °C and 50 °C showed less  
354 significant influence on compressive strength reduction ( $<10\%$ ) for ETC. At the same time,  
355 approximately 30% increase in compressive strength was recorded for ETC low temperature of  
356 0 °C. This was evidenced by homogenous morphology with filled pores in the matrix of ETC  
357 and mineral phases remained unaltered under 0 °C.
- 358 • The significant phase transition peak associated with the transition of  $\lambda$ -sulfur ( $S_{\lambda}$ ) at the

359 temperature range of 160-350°C for pure sulfur (S<sub>8</sub>) shifts to 193-312 °C in case of ETC  
360 produced using sulfur. Further, for ETC subjected to high (40°C and 50°C) and low (0°C)  
361 temperatures, changes in the onset and end temperatures were identified to be 166-350°C and  
362 193-322°C, respectively.

### 363 **Acknowledgements**

364 The authors would like to acknowledge the financial support from Institute of Eminence Research  
365 Initiative Project on Extra Terrestrial Manufacturing (ExTeM).

366

### 367 **References**

- 368 1. Carotenuto, G., Romeo, V., Nicola, S. D., Nicolais L., 2013. Graphite nanoplatelet chemical  
369 cross-linking by elemental sulfur. *Nanoscale Res. Lett.* 8, 94.
- 370 2. Cheng, Y., Ji, S., Liu, Y., Liu, J. 2019. High Sulfur Loading in Activated Bamboo-Derived  
371 Porous Carbon as a Superior Cathode for Rechargeable Li–S Batteries. *Arb. J. Chem.* 12(8),  
372 3517-3525.
- 373 3. Davis, G., Montes, C., Eklund, S., 2017. Preparation of lunar regolith based geopolymer  
374 cement under heat and vacuum. *Adv. Sp. Res.* 59, 1872–1885.
- 375 4. Eilene, T., 1982. A primer on sulfur for the planetary geologist. NASA Contractor Report  
376 3594, Grant NAGW-132, Office of Space Science and Applications, Washington, DC, USA:  
377 National Aeronautics and Space Administration, Scientific and Technical Information  
378 Branch. p. 4.
- 379 5. Grugel, R. N., Toutanji, H., 2016. Viability of sulfur “concrete” on the moon: Environmental  
380 considerations. 44th AIAA Aerospace Sciences Meeting 2006, Reno, NV, 6321-6326.
- 381 6. Grugel, R. N., Toutanji, H., 2008. Sulfur “concrete” for lunar applications – Sublimation  
382 concerns. *Adv. Space Res.*, 41 (1), 103-112.
- 383 7. Hu, Z., Shi, T., Cen, M., Wang, J., Zhao, X., Zeng, C., Zhou, Y., Fan, Y., Liu, Y., Zhao, Z.,  
384 2022, Research progress on lunar and Martian concrete, *Const. Build. Mater.*, 343, 128117,  
385 ISSN 0950-0618.
- 386 8. IS 4031 (Part 6)-1988, Method of Physical Test for Hydraulic Cement, Part 6 Determination  
387 of Compressive Strength of Hydraulic Cement other than Masonry Cement, Bureau of Indian  
388 Standards, New Delhi.

- 389 9. Khoshnevis, B., Yuan, X., Zahiri, B., Zhang, J., Xia, B., 2016. Construction by Contour  
390 Crafting using sulfur concrete with planetary applications. *Rapid Prototyp. J.* 22, 848–856.
- 391 10. King, P.L., McLennan, S.M., 2010. Sulfur on mars. *Elements* 6, 107–112.
- 392 11. Mars exploration rover, Jet propulsion Laboratory, California Institute of Technology,  
393 mars.nasa.gov.
- 394 12. Mars. Nasa.gov, NASA Science Mars Exploration 2022: all.
- 395 13. Mills, J. N., Katzarova, M., Wagner, N.J., 2022. Comparison of lunar and Martian regolith  
396 simulant-based geopolymer cements formed by alkali-activation for in-situ resource  
397 utilization. *Adv. Sp. Res.* 69, 761–777.
- 398 14. Montejo, L. A., Sloan, J. E., Kowalsky, M. J., Hassan, T., 2008. Cyclic Response of  
399 Reinforced Concrete Members at Low Temperatures. *J. Cold Reg. Eng.* 22 (3), 79–102.
- 400 15. Montes, C., Broussard, K., Gongre, M., Simicevic, N., Mejia, J., Tham, J., Allouche, E.,  
401 Davis, G., 2015. Evaluation of lunar regolith geopolymer binder as a radioactive shielding  
402 material for space exploration applications. *Adv. Sp. Res.* 56, 1212–1221.
- 403 16. Murgatroyd, C., Hodges, P., 2001. Building on MARS, *Hydrocarbon Eng.*, 6.
- 404 17. Naser, M.Z., 2019. Extraterrestrial construction materials. *Prog. Mater. Sci.* 105.
- 405 18. Naser, M.Z., Chehab, A.I., 2020. Polymers in space exploration and commercialization.  
406 *Polymer Science and Innovative Applications.*
- 407 19. Nash D.B., 1987. Sulfur in vacuum: Sublimation effects on frozen melts, and applications to  
408 Io's surface and torus. *Icarus*, 72(1), 1-34.
- 409 20. Norman, G. N., Alan, E., 1997. *Chemistry of the Elements* (2nd ed.). Butterworth-  
410 Heinemann. ISBN 0080379419.
- 411 21. Pilehvar, S., Arnhof, M., Pamies, R., Valentini, L., Kjøniksen, A.L., 2020. Utilization of urea  
412 as an accessible superplasticizer on the moon for lunar geopolymer mixtures. *J. Clean. Prod.*  
413 247.
- 414 22. Rapp, D., Mungas, G. S., Easter, R. W., Johnson, K. R., 2006. Accessible water on mars and  
415 the moon, *Earth and Space 2006 – 10th Biennial International Conference on Engineering,*  
416 *Construction, and Operations in Challenging Environments*, League City/Houston, TX, 74.
- 417 23. Scheerbaum, G., 2000. In-Situ manufacture of Martian construction materials, *Space*  
418 20002000, 934-940.

- 419 24. Scott, A.N., Oze, C., Tang, Y., O'Loughlin, A., 2017. Development of a Martian regolith  
420 simulant for in-situ resource utilization testing. *Acta Astronaut.* 131, 45–49.
- 421 25. Steudel. R., 2003. Elemental Sulfur and Sulfur-Rich Compounds II. *Topics in Current*  
422 *Chemistry.* 231, 1-228.
- 423 26. Toutanji, H., Glenn-Loper, B., Schrayshuen, B., 2005. Strength and durability performance of  
424 waterless lunar concrete, 43rd AIAA Aerospace Sciences Meeting and Exhibit, 2005, p. 1436.
- 425 27. Toutanji, H., Grugel, R.N., 2008. Mechanical Properties and Durability Performance of  
426 Waterless Concrete. *Earth & Space 2008: Engineering, Science, Construction, and Operations*  
427 *in Challenging Environments,* 1-8.
- 428 28. Troemner, M., Ramyar, E., Marrero, R., Mendu K, Gianluca, C., Marscrete, 2021. A Martian  
429 concrete for additive construction Application utilizing in situ resources. *Earth and space,*  
430 *ASCE.*
- 431 29. Wan, L., Wendner, R., Cusatis, G., 2016. A novel material for in situ construction on Mars:  
432 experiments and numerical simulations. *Constr. Build. Mater.,* 120, 222-231.
- 433 30. Werkheiser, N.J., Fiske, M.R., Edmunson, J.E., Khoshnevis, B., 2015. Development of  
434 additive construction technologies for application to development of lunar/martian surface  
435 structures using in-situ materials. *CAMX 2015 - Compos. Adv. Mater. Expo* 2395–2402.
- 436 31. Zhou, S., Lu, C., Zhu, X., Li, F., 2020. Preparation and characterization of high-strength  
437 geopolymer based on BH-1 lunar soil simulant with low alkali content. *Engineering.*



## **Conflict of Interest**

The authors have no conflicts of interest to disclose.